AIP | Review of Scientific Instruments

Conditions for Optimum Luminosity and Energy Resolution in an Axial Ray Spectrometer with Homogeneous Magnetic Field

Jesse W. M. DuMond

Citation: Review of Scientific Instruments **20**, 160 (1949); doi: 10.1063/1.1741480
View online: http://dx.doi.org/10.1063/1.1741480
View Table of Contents: http://scitation.aip.org/content/aip/journal/rsi/20/3?ver=pdfcov
Published by the AIP Publishing

Conditions for Optimum Luminosity and Energy Resolution in an Axial β-Ray Spectrometer with Homogeneous Magnetic Field

JESSE W. M. DUMOND
California Institute of Technology, Pasadena, California
(Received October 18, 1948)

In a β-ray spectrometer with axial homogeneous magnetic field, it is shown that optimum energy resolution and luminosity are obtained when the trajectories make an angle close to 45° with the field and that an annular resolving slit should be provided at a determined radial and axial location relative to the source. The combined effect of three independent sources of instrumental energy line width is analyzed for the optimum condition. Formulas are given for the optimum dimensions, the energy resolution and the luminosity.

THE improvement recently obtained in the precision of absolute measurement of nuclear energy levels by the direct crystal diffraction of short wave-length nuclear gamma-rays[1] makes it a matter of considerable interest to develop a β-ray spectrometer of high resolving power and high precision comparable to that obtainable in the crystal diffraction method. The low reflecting power of crystals for wave-lengths of order 30 x.u. and less necessitates the use of extremely strong gamma-ray sources and hence practically eliminates this method as an exploratory technique. Its great advantage on the other hand, lies in the high absolute precision which it affords. It thus complements very satisfactorily the qualities of the β-ray spectrometer since the latter instrument has high luminosity but is very difficult to calibrate with absolute precision. The thought here is that if a β-ray spectrometer of sufficiently high resolving power and reproducibility can be designed, its calibration in terms of absolute β-ray energies can be accomplished by utilizing a number of nuclear gamma-ray lines (precisely standardized by the crystal diffraction method) to eject photoelectrons from known and precisely measured electronic energy levels in appropriately selected secondary radiators. The β-ray spectrometer, so calibrated, can then be used for the accurate measurement of both β-ray and gamma-ray energies from a wide variety of sources and the high absolute precision of the crystal diffraction method can thus be propagated over a much wider domain of measurements.

Many types of the β-ray spectrometer exist or have been proposed. Under the auspices of the Office of Naval Research[2] S. Frankel and E. C. Nelson have very recently made a valuable survey of many of these and have discussed their properties. They fall into three general classes.

(*1.*) *Spectrometers in which the central ray of an electron beam or pencil lies in a plane essentially perpendicular to the magnetic field.*—The electrons execute circular orbits which may consist of arcs greater or less than 180° and the field may be uniform or tapered in various ways to obtain various types of focusing. Notable among these is the Siegbahn-Svartholm[3] so-called double-focusing type.

(*2.*) *Spectrometers of the helical focusing type.*—The magnetic field may be approximately uniform (utilizing the field from a long solenoid) or it may be set up by a more-or-less concentrated coil and may merely have axial symmetry. Electrons leave a more or less concentrated source point on the axis at one end and execute paths more or less helical in form passing through various restricting stops and returning to the axis at the other end where they enter the window of a counter. First suggested by Kapitza in 1923 this type, in various modifications, has been used and described by Tricker,[4] Klemperer,[5] Witcher,[6] K. Siegbahn,[7] Deutsch, Elliot and Evans,[8] and T. Lauritsen and R. F. Christy.[9]

(*3.*) *Spectrometers utilizing electrostatic deflection of the β-rays.*—It is pointed out by Frankel and Nelson[2] that for a fast electron whose velocity nearly equals that of light the same curvature may be produced by a magnetic field of 1000 gauss (which is conveniently small) as by an electric field of 300,000 volts per cm (which is uncomfortably large). Such instruments, which possibly have some importance for the formation of images

[1] DuMond, Lind and Watson, "Precision wave-length and energy measurement of gamma-rays from Au^{198} with a focusing quartz crystal spectrometer." Phys. Rev. **73**, 1392 (1948), Jesse W. M. DuMond, "A high resolving power, curved crystal focusing spectrometer for short wave-length x-rays and gamma-rays," Rev. Sci. Inst. **18**, 626 (1947).

[2] Contract N6onr-238 T.O. 5.

[3] K. Siegbahn and N. Svartholm, Nature **157**, 872 (1946); Arkiv. f. Mat. Astr. o. Fysik, **33A**, No. 21 (1946); N. Svartholm, *ibid.*, **33A**, No. 24 (1946).

[4] R. A. R. Tricker, Proc. Camb. Phil. Soc. **22**, 454 (1925).

[5] O. Klemperer, Phil. Mag. **20**, 259 (1940). Klemperer was apparently the first to propose the concentrated coil or "thin magnetic lens."

[6] Clifford M. Witcher, Phys. Rev. **60**, 32 (1941).

[7] Kai Siegbahn, Arkiv. f. Mat. Astr. o. Fysik, **30**, No. 1 (1943); Phil. Mag. **37**, 162 (1946).

[8] M. Deutsch, L. G. Elliot, and R. D. Evans, Rev. Sci. Inst. **15**, 178 (1944). Includes a painstaking analysis of the thin lens type.

[9] T. Lauritsen and R. F. Christy, Phys. Rev. **73**, 536 (1948).

in electron microscopy have therefore not played an important role in β-spectrometry.[10]

The helical focusing type seems so obviously advantageous as regards the utilizable solid angle of β-rays emanating from the source that this was chosen as the object of the first analysis (the one herein presented) to determine the optimum conditions for simultaneous high resolving power and high luminosity. It is not entirely certain, however, that other and radically different types cannot be devised which will be superior to this one and a program of analysis of other types is now being planned.

The choice of a homogeneous magnetic field (rather than the more complicated field from a concentrated coil) for the β-ray spectrometer here described was based on the following considerations. (1) The analysis is considerably simplified. (2) A homogeneous field is not difficult to realize with a high degree of precision by means of a long solenoid. (3) Small geometrical distortions of such a field by external magnetic influences are more readily detected than they would be in the case of more complicated fields. (4) Since the applied magnetic field is everywhere uniformly strong over the useful region, errors from external magnetic effects are everywhere at a minimum. (5) The adjustment of the spectrometer relative to the field coil is less critical since it depends in first approximation only on the orientation and not on the position. This is a consideration which becomes important because of the high accuracy sought. As Frankel and Nelson[2] point out the thin lens β-spectrometer is more efficient as regards the cost for copper and for power than the solenoid type with uniform magnetic field, but Lauritsen and Christy[9] have shown it to have a poorer resolution for the same range of angles within which the β-rays emanate from the source. The thick lens spectrometer is a compromise between the superior resolving power of the solenoid type and the cheaper thin lens type.

It is a rather surprising fact that the use of a ring shaped annular resolving slit in this type of spectrometer was not suggested until rather recently[11] although the existence of a ring-shaped focus for the bundle of β-rays appears to have been clearly apparent in earlier papers. In a homogeneous magnetic field (solenoid) a bundle of β-rays *of specified energy* leaving a source point on the axis of the spectrometer at colatitude-angles θ in the range $\theta_1<\theta<\theta_1+d\theta$ will focus in a ring whose plane is normal to the axis and whose radius and distance from the source can be readily calculated. It is this type of focusing with which we shall be concerned in this paper.

The trajectory of an electron in a uniform magnetic field is a helix. Let us consider a point source S from which electrons of definite kinetic energy, T, emanate with equal probability in all directions in space. Let us measure the kinetic energy of these electrons in terms of the dimensionless parameter, $\epsilon=T/(m_0c^2)$ (ratio of the kinetic energy to the electron rest-energy, 0.5108 Mev). As x-axis we take a line through the point source S in the direction of the magnetic field whose intensity is H. Let the angle between the helical trajectory and the magnetic field be θ. After one complete turn of the helix the trajectory will once more intersect the x axis in a point S'. Let the diameter of the helical trajectory be R and the distance SS' be L. Then, if e is the electronic charge it is easy to show by elementary considerations that

$$R=2(m_0c/He)[(\epsilon+1)^2-1]^{\frac{1}{2}}\sin\theta, \qquad (1)$$

$$L=2\pi(m_0c/He)[(\epsilon+1)^2-1]^{\frac{1}{2}}\cos\theta. \qquad (2)$$

For brevity let $K=2(m_0c/He)$ and $Q=K[(\epsilon+1)^2-1]^{\frac{1}{2}}$. The assemblage of helical trajectories emanating from S form a triply infinite family of helices characterized by the three parameters; (1.) the azimuth angle of the trajectory at S, (2.) the colatitude angle θ at S, and (3.) the parameter Q depending on the kinetic energy ϵ and the field strength H.

If we consider the entire sub-class of trajectories having a specified value $\theta=\theta_1$ and $Q=Q_1$ but all values of the azimuth angle at S, these helices will all be found to lie on a cigar shaped surface of revolution having the x axis as axis of revolution and having a sinusoidal profile or trace on a plane through the x axis. Figure 1 illustrates a side view of this surface of revolution with a few of the individual helices traced upon it. Only the part of each helix on the side of the surface of revolution toward the observer is drawn, to avoid confusion. The trace or intersection of this surface of revolution with a plane through the x axis will henceforth be designated simply by the word "trace," and the cartesian coordinates x and y describing the equation of a trace will be taken in a plane through the x axis at any arbitrary azimuth angle. Clearly the angle made by the trace at the origin S with the x axis is equal to θ, since there is one of the helical trajectories which is tangent to the trace at S. We shall henceforth be much more concerned

[10] Relatively little attention, however, has been paid to the possibilities of combining electrostatic and magnetic deflections for β-spectrometry.

[11] The suggestion appears to have been first made by Witcher, (see reference 6) who did not, however, make the most of this very ingenious idea. In a letter to the editor of the Physical Review by S. Frankel, Phys. Rev. **73**, 804 (1948) the large gain in solid angular luminosity for a specified high resolution obtainable by this ring focus is explained and emphasized. In a still more recent letter to the Physical Review, E. Persico gives his conclusions as to the optimum finite source size and angle of electron departure from the source. E. Persico, Phys. Rev. **73**, 1475 (1948).

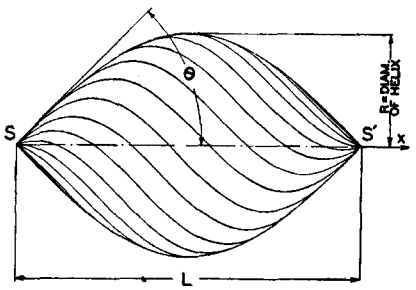

FIG. 1. Illustrating that a family of helical trajectories of specified θ and Q lie on a sinusoidal surface of revolution. L is one full turn of the helix.

with the traces than with the helices. The general equation of a trace is

$$y = Q \sin\theta \sin[x/(Q\cos\theta)]. \tag{3}$$

The traces starting from the origin S form a doubly infinite family of sinusoids characterized by the parameters Q and θ. Now suppose we hold the kinetic energy of the particles and the magnetic field intensity constant (i.e., Q constant) and impose a slight variation on θ. Two closely adjacent traces for a slight variation of θ will be found to have an ultimate intersection point P which will not be situated at S' but somewhere between S' and the summit of the sinusoidal trace. Figure 2 shows the geometry of two such adjacent traces. Let us compute the coordinates x_i and y_i of this ultimate intersection point, by equating

$$Q\sin(\theta+d\theta)\sin\frac{x_i}{Q\cos(\theta+d\theta)} = Q\sin\theta\sin\frac{x_i}{Q\cos\theta}.$$

A straightforward calculation rejecting terms of higher order than the first gives

$$x_i = (Q_1\cos\theta_1)\psi_i, \tag{4}$$

$$y_i = (Q_1\sin\theta_1)\sin\psi_i. \tag{5}$$

Here Q_1 and θ_1 are the particular values of Q and θ which characterize the traces having the ultimate intersection at x_i, y_i, while ψ_i is an angle related to θ_1 by the transcendental equation

$$-\psi_i\tan^2\theta_1 = \tan\psi_i. \tag{6}$$

In Fig. 3 we plot the various branches of the curve $\tan\psi_i$ and also the straight locus $-\psi_i\tan^2\theta_1$. The intersections of these two loci give the solutions for ψ_i, the solution of interest to us being that one which lies in the range $\pi/2<\psi_i<\pi$. Clearly when

$$\theta = 0, \quad \psi_i = \pi,$$

and when

$$\theta = \pi/2, \quad \psi_i = \pi/2.$$

By substituting a series of values of ψ_i between these limits it is an easy matter to calculate the corresponding values of θ, from the equation

$$\tan^2\theta_1 = -(\tan\psi_i/\psi_i), \tag{7}$$

and the curve of Fig. 4 has been traced in this way. Table I gives the relation between ψ_i and θ_1 numerically.

Geometrically ψ_i is the abscissa coordinate *in angular measure* of P the ultimate intersection point, that is

$$\psi_i = x_i/(Q_1\cos\theta_1). \tag{8}$$

(The half-wave-length L of the sinusoidal trace is $\pi Q_1\cos\theta_1$.)

The ultimate intersection point P on the sinusoidal trace is obviously the focal place where the ring focus defining slit should be located in order to select a specified small band of kinetic energies. Clearly this slit must be an annular opening de-

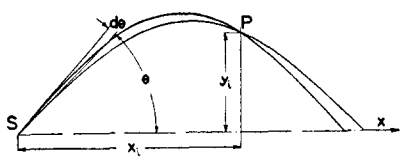

FIG. 2. Showing how two adjacent traces of constant Q but slightly different θ determine an ultimate intersection point P.

fined by a pair of diaphragms normal to the x-axis of the instrument.[12] We shall return later to a more careful consideration of the choice of the width of this opening. Its mean radius is given by y_i (Eq. (5)). In Fig. 5 we show a family of different sinusoidal trace-pairs for one and the same initial angle θ_1 but different values of Q_1 (i.e., different kinetic energies or magnetic field intensities). The ultimate intersection points are seen to lie along a straight line which also passes through the origin S.[13]

We now attack the problem of selecting the best value of θ_1, the colatitude angle at which the β-rays to be used in the instrument are to issue from the source S. If we fix the two points S and P on a certain sinusoidal trace T_1 characterized by the parameters Q_1 and θ_1, P being the ultimate intersection point for T_1 with coordinates x_i, y_i given in Eqs. (4) and (5), and then consider the family of other sinusoidal traces which also pass through S and P in the neighborhood of the trace T_1, these will be characterized by parameters θ and Q in such a way as to establish a functional dependence between these two parameters. For these neighboring traces, as θ departs from θ_1 Q will depart from Q_1, but since the point P *was purposely selected as an ultimate intersection* for the trace T_1 (with its immediate

[12] S. Frankel (see reference 11) recommends that the defining edges of the diaphragms lie on a cone with vertex at the source and axis parallel to the magnetic field.

[13] This line is an element of the cone referred to by Frankel (see references 11 and 12).

neighbors) we have good reason to expect that the departure of Q from Q_1 corresponding to a specified departure of θ from θ_1 *will be a smaller order of infinitesimal quantity than the latter.* Now what we aim to do is to select θ_1 in such a way that, for small deviations $d\theta$ on either side thereof, the largest possible solid angle at the source S results in the smallest possible inhomogeneity of kinetic energy. To do this we substitute the coordinates x_i, y_i of the ultimate intersection point into the general equation of the sinusoidal trace. This gives us

$$\frac{Q_1 \sin\theta_1}{Q \sin\theta} \sin\psi_i = \sin\left(\frac{Q_1 \cos\theta_1}{Q \cos\theta} \cdot \psi_i\right). \qquad (9)$$

Equation (9) is the implicit expression of the above mentioned relationship between Q and θ which obtains for the family of traces passing through the points S and P. We must remember that ψ_i is a function of θ_1 but not of θ. The *solid angle* of β-rays emanating from the source point S is what we wish to maximize or more significantly still *the fraction of the total sphere* into which the β-rays can be projected. Let us define $d\phi$ as this fraction of the total sphere. Then

$$d\phi = \tfrac{1}{2} \sin\theta d\theta. \qquad (10)$$

Since we are only interested in small deviations of θ away from θ_1 and of Q away from Q_1 we define

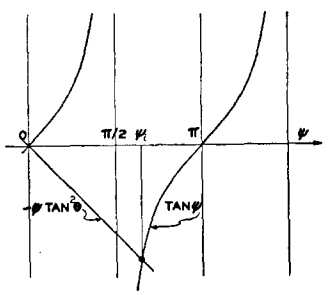

FIG. 3. Graphical solution of the equation relating ψ_i and θ.

two small dimensionless quantities r and δ as follows:

$$\frac{Q-Q_1}{Q_1} = r \ll 1; \quad \frac{\cos\theta - \cos\theta_1}{\cos\theta_1} = \delta \ll 1.$$

We may confidently expect r to be an infinitesimal, at least one order of magnitude smaller than δ for the reason explained previously. Rejecting infinitesimals of higher order than the second, one obtains

$$\frac{Q_1}{Q}\frac{\sin\theta_1}{\sin\theta} = 1 + \frac{\delta}{\tan^2\theta_1} + \frac{1}{2}\frac{\delta^2}{\tan^2\theta_1} + \frac{5}{4}\frac{\delta^2}{\tan^4\theta_1} - r,$$

and $(Q_1/Q)(\cos\theta_1/\cos\theta) = 1 - \delta + \delta^2 - r$.

Substituting these values into Eq. (9) and solving for r one obtains

$$r = \tfrac{1}{4} \cos^2\theta_1 [6 + (5/\tan^2\theta_1) + 2\psi_i^2 \tan^2\theta_1] \delta^2; \qquad (11)$$

now since

$$\delta = \frac{\cos\theta - \cos\theta_1}{\cos\theta_1} \cong \left[\frac{d(\cos\theta)}{\cos\theta_1}\right]_{\theta_1},$$

and $d\phi = \frac{1}{2} \sin\theta d\theta$, we obtain $d\phi^2 = \frac{1}{4}(\cos^2\theta_1)\delta^2$. So that Eq. (11) becomes

$$r = \left[6 + \frac{5}{\tan^2\theta_1} + 2\psi_i^2 \tan^2\theta_1\right](d\phi)^2. \qquad (12)$$

This shows that our prediction was correct, i.e., that r is indeed a smaller order of infinitesimal than δ or than $d\phi$.

Clearly if we are to minimize the inhomogeneity of kinetic energy we must minimize r. In fact calculation shows that for constant field H

$$d\epsilon/\epsilon = [(\epsilon+2)/(\epsilon+1)]r. \qquad (13)$$

Our problem is thus reduced to the evaluation of the bracket of Eq. (12),

$$B(\theta_1) = 6 + 5 \cot^2\theta_1 + 2\psi_i^2 \tan^2\theta_1$$

which is a function of θ_1 only (since ψ_i is a function of θ_1 see Eq. (6). Figure 6 shows the value of this bracket $B(\theta_1)$ plotted as a function of θ_1 and

TABLE I.

ψ_i Degrees	ψ_i Radians	θ_1 Degrees
90	1.571	90°
91	1.588	80°30′
92	1.606	76°40′
93	1.623	73°40′
94	1.641	71°20′
99	1.73	63°20′
108	1.886	52°00′
117	2.041	44°25′
126	2.20	38°20′
135	2.358	33°10′
144	2.513	28°20′
153	2.671	23°30′
162	2.829	18°40′
171	2.984	13°00′
180	3.141	0°

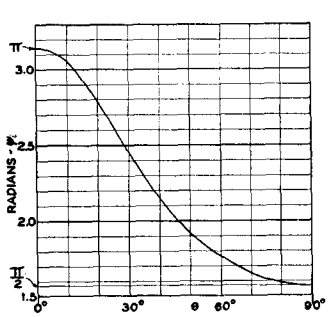

FIG. 4. Graph of ψ_i as function of θ. See also Table I.

Table II gives the numerical values. It was a matter of considerable surprise to the author to discover that $B(\theta_1)$ is very nearly symmetrical about its minimum point and that this latter appears to occur very nearly at $\theta_1=45°$. Neither of the preceding statements is rigorously correct[14] but clearly from the numerical calculations the minimum in B is sufficiently flat to insure that there will be no significant loss of energy resolution if θ_1 is chosen anywhere within the range $40°<\theta_1<50°$. For $\theta_1=45°$ the value of B is about 19. At 40° and 50° it is about 20.

We now pass to the discussion of the appropriate shape and finite extension to give to the source and the appropriate width and disposition of the annular resolving slit. It appears to the author that when an extended source is necessary symmetry considerations dictate a source in the shape of a small very thin flat disk at S normal to and concentric with the x axis since this is the only shape for which all β-particles emerge at the same angle with the surface (45°). The small but unavoidable retardation of those particles which traverse the active layer from different depths will thus be minimized.

It is clear that the β-ray energy spectrum given by the spectrometer will have three[15] independent instrumental sources of line broadening, (1) the "spherical aberration" coming from the use of a finite angular aperture $\theta_1<\theta<\theta_2$, (2) the finite spectral width of the selected energy band determined by the width of the resolving slit at the ring focus, (3) the radius of the source disk which we shall denote by ρ. Each of these sources of broadening alone would, if the effect of the other two were reduced to negligible proportions, yield its own characteristic spectral line profile (corresponding to a sharp line in the true energy spectrum). Figure 7 shows the shapes of these three profiles. With all three sources of broadening operating simultaneously the instrumental spectral line profile will be the *fold* of the three characteristic profiles, each with its own peculiar width parameter (determined by the stops and the source radius ρ selected). This resultant (folded) profile will have a resultant width parameter which will determine the resolving power of the instrument. At the same time, each of the three above mentioned sources of broadening contributes its factor to the counting rate of the instrument. The counting rate is in fact jointly proportional to the area of the source disk (ρ^2), to the width of the energy band selected at the ring focus (we assume, sufficiently high resolution so that all the spectral distributions studied can be regarded as continua) and to the solid angle defined by the aperture stops.[16]

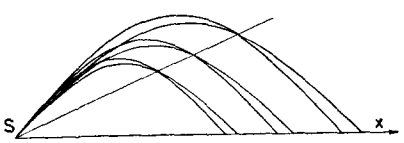

FIG. 5. A family of different trace pairs for the same initial angle θ_1 but different Q, i.e., different energies or magnetic intensities.

TABLE II.

θ_1 Degrees	B
0	∞
10°	167.6
20°	45.8
30°	25.0
40°	19.62
50°	20.0
60°	26.5
70°	48.2
80°	169.2
90°	∞

The problem we must pose is how to apportion the line broadening effects of the above mentioned three causes so as to minimize the resultant line breadth while maximizing the counting rate. The problem is complicated by the curious way in which the width parameter of the resultant folded profile is related to the width parameters of each of the three components.

A brief discussion and justification of the three component profiles of Fig. 7 is first in order. The profile I coming from the finite aperture angle has an infinite ordinate at $\epsilon=\epsilon_0$ but a finite area under the curve since the curve follows an inverse half-power dependence on $\epsilon-\epsilon_0$. This last may be shown as follows: Equation (12) implies that, for angles θ (of β-ray departure) differing slightly from θ_1, the energy ϵ selected by an infinitesimally small ring focus slit (of appropriate position and radius to focus an infinitesimal bundle of rays of angle θ_1)

[14] The value of θ_1 which makes $B(\theta_1)$ a minimum can be easily obtained by expressing B as a function of ψ_i,

$$B=6-\psi_i(5\cot\psi_i+2\tan\psi_i).$$

The minimum of this function occurs at $\psi_i=117.5$ degrees and substituting this value into Eq. (7) one obtains the corresponding value of $\theta_1=44°4'$ as the minimum point of $B(\theta_1)$. This differs slightly but not significantly, from the value 42°20′ given by Persico (see reference 11). It is so close to 45° that we shall use the latter value in design calculations since there is a gain in simplicity by this choice.

How nearly the function $B(\theta_1)$ is symmetric can be appreciated from the fact that even where B is enormous near $\theta=0$ and again near $\theta=\pi/2$, i.e., for vanishingly small angles η, $B(\eta):B(\pi/2-\eta)=5:\pi^2/2$.

[15] A fourth source of broadening coming from the finite *thickness* of the source is here ignored.

[16] The radius of the source disk has an important influence on the counting rate chiefly *in the case of direct sources of β-rays*. It is to such cases that the remainder of the discussion in this article primarily applies. When the primary source is a gamma-ray source which is to eject secondary β-rays from a converter it may be that the counting rate will not increase with the size of the secondary β-ray source. Then only the causes I and II (of line broadening) enter into the discussion.

will differ from ϵ_0 in first approximation by an amount proportional to $(\theta-\theta_1)^2$. This is illustrated by the parabolic characteristic of Fig. 8. If k_1 is a positive constant

$$(\epsilon-\epsilon_0)=k_1(\theta-\theta_1)^2. \tag{14}$$

Now dj the flux of β-particles for small deviations of θ away from θ_1 will be proportional to the zone width $d\theta$ inside of which they are emitted. Differentiating Eq. (14) gives

$$d\theta=\tfrac{1}{2}k_1(\epsilon-\epsilon_0)^{-\frac{1}{2}}d\epsilon \tag{15}$$

which proves the asserted inverse half power dependence of β-particle intensity j on $\epsilon-\epsilon_0$. The base width A_1 in Fig. 7 over which this distribution extends is fixed by the finite range of angle $2\Delta\theta$ for which the angular aperture stop is set. From Eq. (12) it is easy to show that to first-order this base width is given by,

$$A_1=(\Delta\epsilon)_1=[\epsilon(\epsilon+2)/(\epsilon+1)]B(\theta_1)\tfrac{1}{4}\sin^2\theta_1(\Delta\theta)^2. \tag{16}$$

The origin of the profile *II* of Fig. 7 is obvious. If we consider β-rays emanating from a fixed point in the source, say the center, at a fixed sharply defined angle θ_1, then a ring focus slit of narrow but finite width can be considered divided into adjacent infinitesimal elementary rings by each of which slightly different β-ray energies are selected. Energy and position in the slit are linearly related. Because of the narrowness of the entire slit the β-ray flux per unit width of ring and per unit small energy domain will thus be constant across the slit opening yielding the rectangular characteristic shown. The following formula may be readily derived from Eq. (4) and (5) to give the base width A_2 of the rectangular characteristic in terms of the ring focus slit geometry

$$A_2=(\Delta\epsilon)_2=K^{-1}(\sin\psi_i\sin\theta_1)^{-1}\times(\epsilon+1)^{-1}\epsilon^{\frac{1}{2}}(\epsilon+2)^{\frac{1}{2}}\Delta y_i; \tag{17}$$

$$=K^{-1}(\psi_i\cos\theta_1)^{-1}(\epsilon+1)^{-1}\epsilon^{\frac{1}{2}}(\epsilon+2)^{\frac{1}{2}}\Delta x_i. \tag{18}$$

$$K=2(m_0c/He)$$

Δy_i and Δx_i are, respectively, the radial and axial widths of the ring focus slit which in formulas 17 and 18 is assumed to have its outer and inner edges lying on the cone whose vertex is at the source in the way first suggested by Frankel,[11] see Fig. 9.

The finite size of the source disk yields the semi-elliptical line profile shown in Fig. 7 at *III*. This conclusion is arrived at as follows: Consider for the moment the trajectories of β-rays which pass through a single point P in the ring focus slit and which take off from the source under a well defined angle θ. Set up cartesian coordinates ξ and η on the source disk with origin at the center such that the η-axis lies in the axial plane through P and the ξ-axis is perpendicular thereto. If now we displace the source point over the source in the η-direction holding θ and P fixed the energy selected will vary for, small displacements, substantially linearly with the displacement because a radial displacement η at the source with P fixed produces the same result as holding the source point fixed and executing a radial displacement $-\eta$ of the point P. On the other hand small displacements of the source point along the ξ-axis will result in no first-order variation whatever of the energy selected because such displacements are equivalent to holding the source point fixed and displacing P tangentially in the ring focus slit. Thus if the source disk is explored holding the point P and the angle θ constant a contour map of lines of constant selected energy can be plotted on the disk and these will simply be a set of equidistant straight lines parallel to the ξ-axis. If ϵ_0 is the energy selected when the source point is at the center of the disk, then each differential energy domain will have associated with it a flux of β-rays proportional to the area between two of the adjacent parallel contours, that is to say proportional to the length of one of the chords of the circle while the distance of the chord from the center is proportional to $\epsilon-\epsilon_0$ as indicated in Fig. 10. Thus, the flux of β-rays per unit spectral energy interval will obey a law

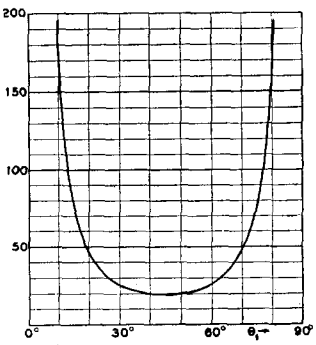

FIG. 6. The bracket $[6+5\cot^2\theta_1+2\psi_i^2\tan^2\theta_1]$ plotted as a function of θ_1. See also Table II.

$$y=k_3[A_3^2-(\epsilon-\epsilon_0)^2]^{\frac{1}{2}} \tag{19}$$

which is in general the elliptical profile shown at *III* in Fig. 7. The half-width of this profile at the base is A_3 and is given in terms of the radius ρ of the source disk by the formula

$$A_3=(\Delta\epsilon)_3=K^{-1}(\epsilon+1)^{-1}\epsilon^{\frac{1}{2}}(\epsilon+2)^{\frac{1}{2}}\times(\sin\psi_i-\psi_i\cos\psi_i)^{-1}(\sin\theta_1)^{-1}\rho. \tag{20}$$

A few remarks are now in order regarding the validity of *folding* the three profiles of Fig. 7 to obtain the resultant instrumental line profile. For this to be a strictly valid procedure the shape of each profile must be completely independent of changes in the variables upon which the other two profiles depend. Thus, for example, as we vary ξ and η in our exploration over the surface of the source disk

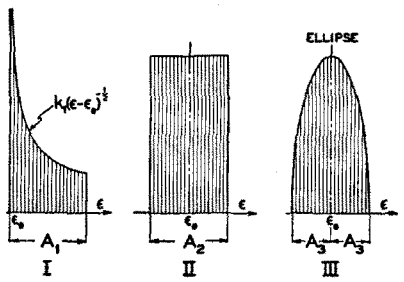

FIG. 7. Illustrating the three spectral profiles introduced by, (I) Finite angular aperture, (II) Finite width of ring focus slit, and (III) Finite size of source disk.

holding the point P in the ring focus slit stationary, is it possible by means of appropriate stops to insure that θ will also remain essentially constant as we have supposed it does in the above derivation of the elliptical profile? The answer is affirmative to a first approximation from the following reasoning. We suppose, to simplify the argument, that the diaphragm opening which selects the range of values, $\theta=\theta_1\pm\Delta\theta$, is placed at such a point along the axis of the instrument that the helical β-ray trajectories shall execute just *one-half of a turn*[17] in going from this diaphragm to the ring focus slit. (For a spectrometer in which $\theta_1=45°$ this situates it at about 0.15 the distance from S to S'.) If this is done then displacements of the source point on the source disk along the η direction (direction of greatest rate of change of energy) *produce tangential displacements* of the trajectory in the θ-selecting slit so that θ remains constant to the first order. Furthermore, displacements of the source point over the source disk along the ξ-direction produce changes in the limiting values of θ which can also be shown to affect the value of the energy only to the second order. This arises from the fact that the maximum displacement ρ over the source disk turns out to be small in comparison to the width of the θ-selecting slit for an instrument of reasonably high resolving power such as $\Delta\epsilon/\epsilon=1/1000$. Thus, we are reassured that the instrument affords a means essentially equivalent to holding ρ and the point P fixed while varying ξ and η over the source disk. The other two cases are much more easily perceived and need hardly be discussed beyond a mere statement of each. They are: Hold θ and the source point ξ, η fixed while varying the point P in the ring focus slit. Hold P and the source point ξ, η, fixed while varying θ.

We must now decide what width parameter (of the folded resultant of profiles I, II, III) to choose as a measure of the instrumental resolving power. If we choose *the base width* W_B of the resultant line for this measure, this will be given very simply by summing the base widths of the components, i.e., $W_B=A_1+A_2+A_3$. Now since the counting rate is proportional to the product $A_1^{\frac{1}{2}}A_2A_3^2$, if we wish to maximize this rate while holding $W_B=A_1+A_2+A_3$ at some specified constant value it is a simple matter to show that we must make $A_1=W_B/7$, $A_2=2W_B/7$ and $A_3=4W_B/7$. To the writer, W_B does not seem to be a satisfactory measure of resolving power however. It is too conservative a choice. A much better measure is the *width at half-maximum height* which we shall designate simply as W. To get this we must actually fold profiles I, II, and III together.

It is a well-known fact that the operation of folding several functions together gives a resultant whose shape is independent of the *order* in which the folding operations were performed. Let us fold profiles I and II together first. We shall call the half-maximum width of the resultant, W_{12}. Because of the discontinuous nature of the functions it is necessary to distinguish two cases corresponding, respectively, to $A_1<A_2$ and $A_2<A_1$. Perhaps

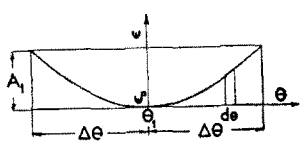

FIG. 8. Dependence of $\epsilon-\epsilon_0$ on $\theta-\theta_1$ from which profile I is derived.

the easiest way to obtain the fold is to decompose profile II into two step functions, one positive the other negative, with a displacement A_2 between the discontinuities. The fold of each step function into the inverse half-power curve then gives a parabola with horizontal axis. By such reasoning we obtain the results shown in Fig. 11. The case $A_2<A_1$ breaks into two sub-cases according to whether $A_2<(16/25)A_1$ or $(16/25)A_1<A_2<A_1$. For the latter sub-case the half-maximum width becomes $W_{12}=A_2+A_1-(A_2A_1)^{\frac{1}{2}}$. This then is the sub-case within which the half-maximum width makes the transition from its lower boundary value A_2 to its upper boundary value $21A_2/16$. The important thing to notice about this bizarre behavior of the half-maximum width W_{12} is that it remains within the very narrow range, $A_2<W_{12}<21A_2/16$, *both upper and lower bounds of which are independent of* A_1 *no matter how large* A_1 *may become.* Since the counting rate is proportional to $A_1^{\frac{1}{2}}$ one might at first be tempted, by greatly increasing the half aperture angle $\Delta\theta$, to make A_1 very large indeed since it will not result in any increase in the half maximum width W_{12}. This however would be unwise because such an increase in A_1 merely *adds intensity by lengthening the tail* of the line to the

[17] One-half turn of the helical trajectory corresponds to one-quarter turn round the principal axis of the instrument since the latter is on the circumference, not on the axis of the helix. This choice of position for the θ-selecting slit simplifies the discussion but is not to be regarded as imperative. The point where the two extreme traces of the pencil are radially farthest apart might be an even better place to locate it.

right (Fig. 11). That part of the line which is useful in resolving it from other lines is the core or essentially the part inside the two half-maximum points and as A_1 increases (A_2 constant) there is no gain in the intensity associated with this core beyond the point $A_1=A_2$. Increasing A_1 beyond the value A_2 therefore merely adds to the background distortion in an objectionable way without usefully increasing the intensity of the core of the line. On the other hand as A_1 is decreased below A_2 the intensity associated with the core of the line diminishes. We conclude therefore that the optimum is probably achieved if $A_1=A_2$ in which case the line assumes the simple form shown in the second diagram from the top of Fig. 11. It is this profile then which we shall fold with the elliptical profile *III* of Fig. 7.[18]

Four values of the ratio A_3/W_{12} have been selected for plotting namely, $A_3/W_{12}=0.5$, 0.75, 1.00, 1.25. In each case the folded profile has been plotted and W the width at half-maximum has been determined in terms of $W_{12}=A_1=A_2$. If we think of the half maximum width W as held constant we can thus express the three width parameters A_1, A_2, A_3, of Fig. 7 as multiples of W for the case of each of the four ratios A_3/W_{12} chosen. Now the total counting rate will be proportional to the product $A_1{}^{\frac{1}{2}}A_2A_3{}^2$ as we have already stated so that it is possible to compute a number which will be proportional to the total counting rate for constant W as a function of various ratios A_3/W_{12}. Table III shows the data with which this has been done.

In Fig. 12 we show the numbers (proportional to counting rate) in the last column of Table III plotted as a function of A_3/W_{12}. It seems clear that the optimum value occurs somewhere very close to $A_3/W_{12}=1$ or in other words the condition $A_1=A_2=A_3$ in all probability comes very close to giving the greatest counting rate for the least resultant width at half maximum. In Fig. 13 we show the resultant optimum line profile to be expected under this condition. Note that this profile has a width at half maximum which is 1.62 times each of the three equal parameters A_1, A_2, or A_3. Only a slight vestige of the asymmetry which results from the influence of the profile *I* can be detected when we examine Fig. 13. The width parameter $A_1=A_2=A_3$ is shown to scale in the figure.

The author makes no claim that the above analysis for the optimum relationship between the parameters A_1, A_2, and A_3 is highly rigorous. He is well aware that the procedure of first choosing the optimum condition $A_1=A_2$ using the width W_{12} as a criterion *before* folding *I* and *II* into *III* is strictly open to criticism. The condition $A_1=A_2=A_3$ is not here laid down as giving *accurately* the greatest intensity for a specified resolving power. It seems likely however that it defines the optimum condition so closely that no significant gain in intensity would be effected by modifying it.

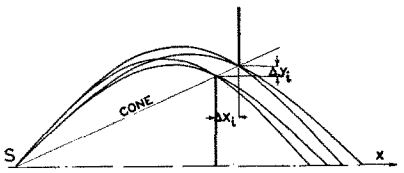

FIG. 9. Showing geometry of ring focus slit with its edges lying on a conical surface with vertex at S.

The radius ρ of the source disk should obviously then be chosen so that the loss of energy resolution A_3 from this cause alone shall be equal to A_1 the loss of energy resolution from the solid angle $d\phi$ (or from the range $\Delta\theta$) given in Eq. (16) also the width of the ring focus slit should be chosen to make $A_2=A_1$ using Eqs. (17) and (18) to proportion the radial and axial spread of the slit. The condition $A_3=A_1$ gives the following formula for the radius of the source disk

$$\rho=K\epsilon^{\frac{1}{2}}(\epsilon+2)^{\frac{1}{2}}B(\theta_1)(\sin\theta_1)\times(\sin\psi_i-\psi_i\cos\psi_i)(d\phi)^2;\quad K=\frac{2m_0c}{He}. \tag{21}$$

For the optimum design with $\theta_1=45°$ and $\psi_i=2.03$ rad., this gives

$$\rho=36R(d\phi)^2 \tag{22}$$

in which

$$R=\sqrt{2}(m_0c/He)[(\epsilon+1)^2-1]^{\frac{1}{2}}. \tag{23}$$

R is the maximum radial distance of the median traces from the axis of the instrument. We shall take it as a convenient geometrical unit in terms of which all the other linear dimensions are to be expressed.

The condition $A_2=A_1$ leads to the following formulas for the dimensions of the ring focus slit,

$$\Delta y_i=K\epsilon^{\frac{1}{2}}(\epsilon+2)^{\frac{1}{2}}\sin\psi_i\sin\theta_1B(\theta_1)(d\phi)^2, \tag{24}$$

$$\Delta x_i=K\epsilon^{\frac{1}{2}}(\epsilon+2)^{\frac{1}{2}}\psi_i\cos\theta_1B(\theta_1)(d\phi)^2. \tag{25}$$

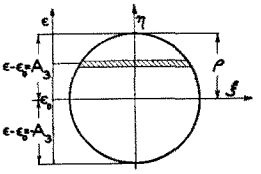

FIG. 10. Iso-energy bands and coordinates ξ, η on the source disk. To illustrate derivation of profile *III*.

[18] If the case in point is one in which the finite radius of the source disk plays no part in giving an increased counting rate (γ-ray sources for example) so that the loss of resolving power from cause III can be kept small in comparison to that from causes I and II without any sacrifice of counting rate, then the discussion from this point on concerning the effect of folding in the elliptical profile *III* should be ignored and the final profile will be essentially the second one from the top in Fig. 11 with the width at half maximum height $W=W_{12}=A_1=A_2$.

For the optimum design with $\theta_1=45°$ and $\psi_i=2.03$ radians these become

$$\Delta y_i=18R(d\phi)^2, \tag{26}$$

$$\Delta x_i=41R(d\phi)^2. \tag{27}$$

Clearly, for a given energy ϵ, Eq. (23) shows that we may take R as large as we please provided we can make H small in inverse proportion. There is an advantage in large dimensions because by Eq. (22) ρ is proportional to R and hence the utilizable area and strength of source increases as ρ^2 and R^2. The practical limit to this occurs either when the cost becomes prohibitive or when H must be made so small that uncontrollable outside magnetic influences disturb the field distribution intolerably.

Figure 14 is a schematic axial section through the instrument showing its geometry and the nomenclature of its principal dimensions. We append below a list of the principal useful formulae and relations for the optimum case of $\theta_1=45°$, the nomenclature being that indicated in Fig. 14. Attention is called to the θ-selecting stop that is required to define the two extreme traces on either side of the median trace ($\theta_1=45°$). This is placed one-half turn of the helical β-ray trajectory nearer to the source than the ring focus slit.[17] Other stops which do not define the beam but serve merely to reduce scattering will doubtless be found advantageous. A heavy lead core to protect the counter from gamma rays is also commonly provided. These are omitted however in Fig. 14.

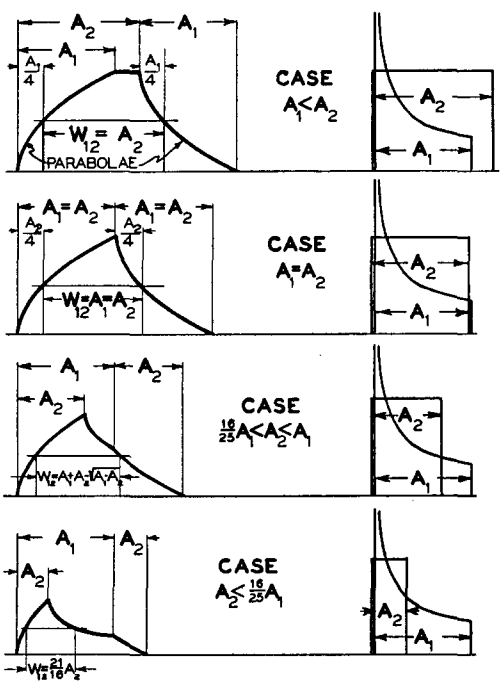

FIG. 11. Illustrating the various cases which arise when profiles *I* and *II* of Fig. 7 are folded together. In the above figure A_2 has been progressively diminished holding A_1 constant. The component profiles are shown in each case on the right, the folded resultant on the left. Note that the half-maximum width W_{12} of the folded resultant never becomes less than A_2 or greater than $(21/16)A_2$.

TABLE III. Case of $W_{12}=A_1=A_2$.

A_3/W_{12}	W	$A_1=A_2$	A_3	$A_1^{\frac{1}{2}}A_2A_3^2$
0	1.00 W_{12}	1.00 W	0	0
0.50	1.19 W_{12}	0.84 W	0.420 W	0.135
0.75	1.40 W_{12}	0.714 W	0.535 W	0.173
1.00	1.62 W_{12}	0.617 W	0.617 W	0.185
1.25	2.00 W_{12}	0.500 W	0.625 W	0.138
∞	A_3	0	1.000 W	0

Resume of Formulas for Optimum β-Spectrometer Design ($\theta_1=45°$)

Fundamental Radius

$$R=\tfrac{1}{2}\sqrt{2}Q_1=\sqrt{2}(m_0c/He)[(\epsilon+1)^2-1]^{\frac{1}{2}}. \tag{28}$$

Luminosity or Utilizable Fraction of all β-emissions

$$d\phi=\tfrac{1}{2}\sin\theta_1 d\theta_1. \tag{29}$$

Energy Uncertainty Parameter A_1 Caused by Angular Aperture

$$A_1=(\Delta\epsilon)_1=\epsilon(\epsilon+2)(\epsilon+1)^{-1}20(d\phi)^2. \tag{30}$$

Radius of Source Disk (to make $A_3=A_1$)

$$\rho=40R(d\phi)^2. \tag{31}$$

Radial Width of Ring Focus Slit Opening (to make $A_2=A_1$)

$$\Delta y_i=18R(d\phi)^2. \tag{32}$$

Axial Width of Ring Focus Slit Opening (to make $A_2=A_1$)

$$\Delta x_i=41R(d\phi)^2. \tag{33}$$

Mean Radius of Ring Focus Slit

$$r_s=0.896R. \tag{34}$$

Mean Axial Distance of Ring Focus Slit from Source

$$S=2.03R. \tag{35}$$

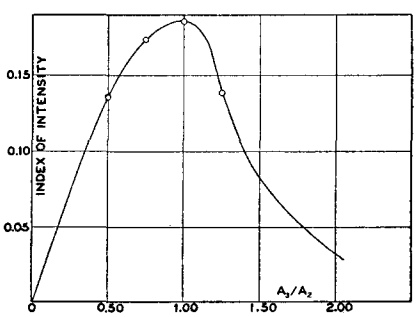

FIG. 12. Curve indicating the optimum ratio of A_3/A_2 to yield maximum intensity for a specified breadth W (at half maximum) of the resultant of the three profiles *I*, *II*, and *III*.

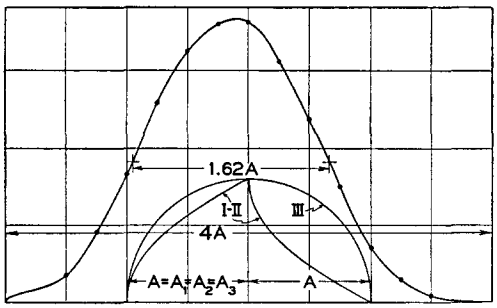

FIG. 13. Resultant instrumental line profile for the optimum case, $A_1=A_2=A_3$. The half-maximum width, W, turns out to be $1.62A$ where $A=A_1=A_2=A_3$. The base width is $4A$. The component profiles I–II (fold of I into II) and III are shown. Profile III may be thought of as the one which moves across profile I–II to give the resultant shown. A vestige of the asymmetry of I–II can be seen in the resultant.

Mean Axial Distance of Counter from Source

$$L=\pi R. \tag{36}$$

Linear Extension of β-Ray Beam on the Axis at the Counter

$$C=2\pi\sqrt{2}Rd\phi. \tag{37}$$

Axial Distance of θ-Selecting Slit from Source

$$A_\theta=0.459R. \tag{38}$$

Mean Radius of θ-Selecting Slit

$$r_\theta=0.444R. \tag{39}$$

Half-Radial Width of θ-Selecting Slit

$$\Delta r_\theta=0.854Rd\phi=2.42Rd\phi. \tag{40}$$

In a magnetic β-ray spectrometer of the type here described if the resolving power is very high the geometrical axis defined by the source and stops must be very accurately aligned parallel with the magnetic field, otherwise the ray traces will not register correctly and simultaneously all around the annular defining slit. For this reason it will be wise to provide for a slight amount of angular adjustment so that the orientation of the vacuum chamber with its source holder, stops and counter can be slightly varied relative to the solenoid which furnishes the magnetic field.

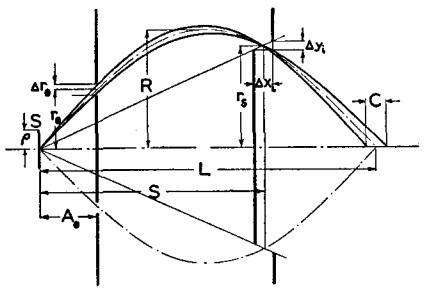

FIG. 14. Schematic axial section through β-ray spectrometer giving nomenclature of optimum dimensions.

It appears from the present analysis that by adhering to the optimum proportions as indicated above it should be possible to design a β-ray spectrometer with a direct β-ray source in which the utilized fraction of the total sphere around the source is $d\phi=0.01$ and in which for the three cases, $\epsilon\ll1$, $\epsilon=1$, $\epsilon\gg1$, the resolution is given respectively by $\Delta\epsilon/\epsilon=0.0065$, 0.0049, 0.0032 wherein $\Delta\epsilon$ is the full instrumental line width at half maximum in ϵ-energy units and ϵ is the energy at which the line occurs expressed as a fraction of the electron rest energy. The radius of the source disk should be for such a case $\rho=0.004R$ where R is the fundamental radius of the instrument (or the maximum radial distance from the central axis attained by the median ray of the pencil of electron trajectories). If the source disk can be made indefinitely small without loss of intensity (case of γ-ray source with converter) then $\Delta\epsilon/\epsilon=0.004$, 0.003, 0.002 for the above three cases.

The author wishes to acknowledge with gratitude very helpful criticisms and discussions of this paper by E. R. Cohen and by Professor R. F. Christy.